

Reparameterization Flow Policy Optimization

Hai Zhong, Zhuoran Li, Xun Wang, and Longbo Huang ^{*}

Institute for Interdisciplinary Information Sciences (IIIS), Tsinghua University
 {zhongh22,lizr20,wang-x24}@mails.tsinghua.edu.cn, longbohuang@tsinghua.edu.cn

Abstract

Reparameterization Policy Gradient (RPG) has emerged as a powerful paradigm for model-based reinforcement learning, enabling high sample efficiency by backpropagating gradients through differentiable dynamics. However, prior RPG approaches have been predominantly restricted to Gaussian policies, limiting their performance and failing to leverage recent advances in generative models. In this work, we identify that flow policies, which generate actions via differentiable ODE integration, naturally align with the RPG framework, a connection not established in prior work. However, naively exploiting this synergy proves ineffective, often suffering from training instability and a lack of exploration. We propose Reparameterization Flow Policy Optimization (RFO). RFO computes policy gradients by backpropagating jointly through the flow generation process and system dynamics, unlocking high sample efficiency without requiring intractable log-likelihood calculations. RFO includes two tailored regularization terms for stability and exploration. We also propose a variant of RFO with action chunking. Extensive experiments on diverse locomotion and manipulation tasks, involving both rigid and soft bodies with state or visual inputs, demonstrate the effectiveness of RFO. Notably, on a challenging locomotion task controlling a soft-body quadruped, RFO achieves almost $2\times$ the reward of the state-of-the-art baseline.

1 Introduction

Reparameterization Policy Gradient (RPG) [49, 32, 15, 56] is a model-based paradigm that reparameterizes the policy’s action distribution as a differentiable transformation from a source distribution [23, 39]. By directly backpropagating gradients through the trajectory, RPG typically exhibits lower variance than likelihood-ratio estimators such as REINFORCE [47], thereby enabling significantly higher sample efficiency [32, 49, 16]. This efficiency has driven recent successes in robotic applications leveraging differentiable simulators, ranging from quadrupeds to quadrotors [28, 55, 18, 41, 35].

However, prior RPG approaches have predominantly focused on Gaussian policies [49, 48, 56], limiting

^{*} Corresponding Author

their expressiveness in modeling complex action distributions. In contrast, flow policies trained via imitation learning have recently demonstrated remarkable success in generating robotic actions [5, 6, 7, 26], owing to their superior expressiveness, implementation simplicity, and fast inference. To overcome the limitations of demonstrations, there has been a surge of research interest in leveraging reinforcement learning (RL) to enable flow policies to learn directly from their own experience [22, 31, 54, 53, 52, 29].

In this work, we identify the key insight that flow policies inherently parameterize a differentiable mapping from source noise to actions, thus naturally aligning with the RPG framework. Leveraging this synergy, we view the flow generation process as an integral part of the rollout trajectory, enabling policy gradients to be computed by backpropagating directly through both the ODE integration and system dynamics—a novel connection not established in prior work. However, directly optimizing flow policies with RPG fails to yield strong performance, primarily due to optimization instability and insufficient exploration.

Hence, we propose **Reparameterization Flow Policy Optimization (RFO)**, an on-policy RL algorithm optimizing flow policies with RPG. Beyond the core RPG mechanism, we introduce two regularization terms crucial for stable training. The first leverages actions sampled during rollouts as targets for Conditional Flow Matching (CFM) to stabilize policy updates, while the second utilizes targets from the uniform distribution to explicitly encourage exploration. Additionally, we propose a variant of RFO incorporating an action chunking mechanism [5, 7, 25] to improve the temporal consistency of generated actions. We evaluate our method across a diverse suite of locomotion and manipulation tasks, involving both rigid and soft bodies, using state or visual inputs. Notably, RFO achieves nearly $2\times$ the reward of the state-of-the-art (SOTA) baseline on a challenging soft-body quadruped locomotion task with a high-dimensional action space (\mathbb{R}^{222}).

RFO represents a significant contribution to both the flow-based RL and RPG communities. From the perspective of flow-based RL, RFO uniquely combines the strengths of distinct paradigms: it inherits the high sample efficiency of RPG while eliminating the need for intractable action log-likelihood computations—benefits typically associated with off-policy methods. Simultaneously, as an on-policy approach, RFO seamlessly integrates with massively parallel differentiable physics simulators, such as Rewarped, DFlex, and Newton [48, 49, 16, 33], to significantly accelerate training. From the RPG perspective, to the best of our knowledge, RFO is the first work to successfully investigate and demonstrate the effectiveness of incorporating state-of-the-art generative flow models.

To summarize, our contributions are threefold: (i) We propose a novel paradigm for training flow policies using Reparameterization Policy Gradients, unlocking high sample efficiency without approximating intractable likelihoods. (ii) We introduce Reparameterization Flow Policy Optimization (RFO), an algorithm equipped with novel regularization mechanisms for stability and exploration, further extended with an action-chunking formulation. (iii) We conduct extensive experiments on differentiable simulators, demonstrating that RFO consistently achieves strong performance across challenging rigid and soft-body tasks compared to existing baselines.

2 Related Work

2.1 Online Reinforcement Learning Algorithms for Flow and Diffusion Policy

Online RL algorithms for flow and diffusion policies can be categorized as off-policy or on-policy. Off-policy algorithms rely on Q-functions to train generative policies [37, 45, 8, 29, 30, 10, 14, 50, 54, 12, 46, 36], offering the advantage of bypassing the calculation of action log-likelihoods. One approach for policy optimization involves backpropagating Q-gradients to the noise prediction or vector field network [44, 45, 29, 46, 54, 8]. This is achieved by reparameterizing the flow or diffusion policy as a transformation from sampled noise to actions, which allows for the direct backpropagation of Q-function gradients through this differentiable transformation to the policy network. Another class of approaches exploits the intrinsic connection between the score function (or velocity field) and Q-functions [37, 14, 2, 12]. For instance, [37] proposes matching the score functions to Q-function gradients. Meanwhile, [14, 30, 12] utilize a Q-weighted regression loss to train the noise prediction network, whereas [10] trains the velocity network via a Q-weighted conditional flow matching loss.

On-policy RL algorithms for flow and diffusion policies [13, 38, 53, 51, 31] must address the challenge of approximating otherwise intractable action log-likelihoods. One prevalent approach is to treat the sampled noise as an augmented state, which enables the calculation of action likelihoods conditioned on the noise. For instance, DPPO [38] constructs a two-level Markov Decision Process that propagates policy gradient signals to each denoising step. Similarly, NCDPO and Reinfflow [51, 53] treat the action generation as a deterministic process by conditioning on all sampled noise, and additionally train a noise injection network to compute action log-likelihoods. Alternatively, FPO [31] approximates action log-likelihoods via the conditional flow matching loss. GenPO [13] introduces a specialized doubled dummy action generation mechanism, which enables the calculation of exact action log-likelihoods. In contrast, RFO entirely bypasses likelihood computation by leveraging reparameterization gradients through differentiable dynamics, which typically yields lower-variance gradient estimates than REINFORCE-like policy gradients [32].

2.2 Reparameterization Policy Gradient

Reparameterization Policy Gradient exploits the reparameterization trick [23, 39, 32] to render the action sampling process differentiable. By defining the action as a deterministic transformation of a noise variable drawn from a fixed source distribution, RPG enables the computation of low-variance policy gradients by backpropagating directly through the system dynamics. These dynamics are typically provided by either differentiable simulators [49, 19, 48] or learned world models [17, 4, 24]. Consequently, RPG generally yields gradient estimates with significantly lower variance compared to likelihood-ratio estimators like REINFORCE [32, 43]. Prominent RPG algorithms, such as SHAC and AHAC [49, 16], further stabilize training by truncating the backpropagation horizon and leveraging value function gradients to estimate long-term returns. While prior work has investigated the use of multimodal policies within RPG [20], the integration of modern expressive generative models—specifically Diffusion and Flow Matching—remains largely unexplored. RFO bridges this gap by introducing the first RPG-based framework tailored for Flow Matching

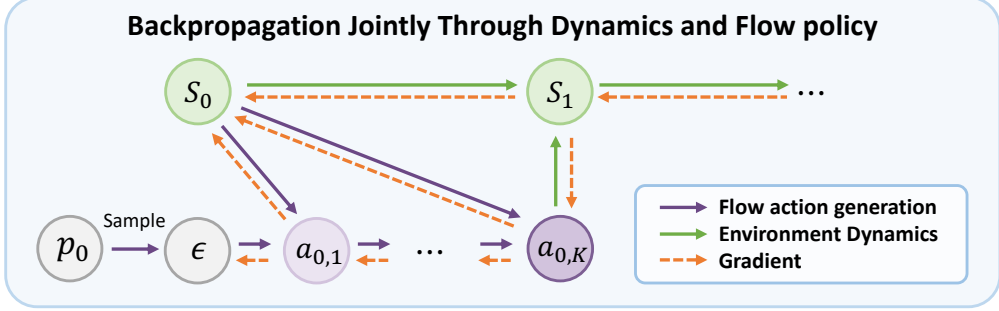


Figure 1: RFO optimizes the flow policy by jointly backpropagating through the dynamics and the flow policy.

policies.

3 Preliminaries

3.1 Reinforcement Learning Problem Formulation

We formulate the reinforcement learning (RL) problem as a Markov Decision Process (MDP) [42], defined by the tuple $(\mathcal{S}, \mathcal{A}, p, r, \rho_0, \gamma)$. Here, \mathcal{S} denotes the state space, and \mathcal{A} denotes the action space. The transition function $p(s'|s, a)$ defines the probability density of transitioning to the next state $s' \in \mathcal{S}$ given the current state $s \in \mathcal{S}$ and action $a \in \mathcal{A}$. The term $r(s, a)$ represents the reward function, ρ_0 denotes the initial state distribution, and $\gamma \in [0, 1]$ is the discount factor. In this work, we consider a continuous and **bounded** action space \mathcal{A} . The objective of RL is to maximize the expected discounted cumulative reward:

$$J(\theta) = \mathbb{E}_{\tau \sim \pi_\theta} \left[\sum_{t=0}^{\infty} \gamma^t r(s_t, a_t) \right], \quad (1)$$

where $\tau = (s_0, a_0, s_1, a_1, \dots)$ denotes a trajectory sampled from the distribution induced by the policy π_θ , with $s_0 \sim \rho_0$.

3.2 Flow Model and Flow Policy

Flow Models and Flow Matching. Flow models [26, 9, 3, 27] constitute a class of generative models that transform samples from a source distribution $x_0 \sim p_0$ (e.g., standard Gaussian) to a target distribution $x_1 \sim p_1$ via an invertible flow map $\phi : [0, 1] \times \mathbb{R}^d \rightarrow \mathbb{R}^d$. This flow map is induced by a time-dependent, neural-network-parameterized vector field $v_\theta(x, u)$ [9], defined by the ordinary differential equation (ODE):

$$\frac{d}{du} \phi(u, x_0) = v_\theta(\phi(u, x_0), u), \quad (2)$$

where $\phi(0, x_0) = x_0$ and u denotes the flow time. To learn the parameterized vector field v_θ , the Conditional Flow Matching (CFM) objective is proposed [26]. Specifically, CFM constructs a linear interpolation path

conditioned on the source noise x_0 and the target sample x_1 , where the intermediate state is given by:

$$x_u = (1 - u)x_0 + ux_1, \quad u \in [0, 1]. \quad (3)$$

Consequently, the CFM objective is defined as:

$$\begin{aligned} \mathcal{L}_{\text{CFM}}(\theta) \\ = \mathbb{E}_{u \sim \mathcal{U}[0,1], x_0 \sim p_0, x_1 \sim p_1} \left[\|v_\theta(x_u, u) - (x_1 - x_0)\|^2 \right], \end{aligned} \quad (4)$$

where $\mathcal{U}[0, 1]$ is the uniform distribution.

Flow Policy. Flow models serve as a powerful policy class for generating actions [5, 22, 7] from potentially complex, multi-modal distributions. To define a state-conditioned policy, the vector field $v_\theta(x, u|s)$ is conditioned on the current state $s \in \mathcal{S}$. An action a is generated by first sampling x_0 from the source distribution p_0 , and subsequently solving the following ODE from $u = 0$ to $u = 1$:

$$\frac{dx}{du} = v_\theta(x, u|s), \quad \text{with } x(0) = x_0. \quad (5)$$

The core challenge in utilizing flow policies for RL lies in propagating reward signals to optimize the vector field v_θ .

3.3 Reparameterization Policy Gradient

The Reparameterization Policy Gradient method builds upon the reparameterization trick [23, 39]. Instead of directly parameterizing a potentially complex, multi-modal action distribution, RPG parameterizes the transformation from a source distribution to the action distribution. Specifically, given noise ϵ sampled from a fixed source distribution, the action a is computed via a transformation function $a = f_\theta(\epsilon; s)$ (typically parameterized by a neural network), conditioned on the state s . Prior RPG-based approaches have predominantly focused on Gaussian policies [49, 16, 48, 15, 56], effectively modeling the transformation from a standard Gaussian distribution to a state-dependent Gaussian distribution.

Following previous RPG work [49, 16, 48], we focus on deterministic environment dynamics $s_{t+1} = g(s_t, a_t)$ and assume environment dynamics and the reward functions are differentiable.

Leveraging the reparameterization transformation, RPG computes the policy gradient by backpropagating through the environment dynamics, utilizing the dynamics Jacobians $\frac{\partial s_{t+1}}{\partial a_t}$ and $\frac{\partial s_{t+1}}{\partial s_t}$. The objective function and its gradient are defined as:

$$J(\theta) = \mathbb{E}_{s_0, \epsilon_0, \epsilon_1, \dots} [R(\tau)], \quad (6)$$

$$\nabla_\theta J(\theta) = \mathbb{E}_{s_0, \epsilon_0, \epsilon_1, \dots} [\nabla_\theta R(\tau)], \quad (7)$$

where $R(\tau) = \sum_{t=0}^{\infty} \gamma^t r(s_t, a_t)$ denotes the cumulative discounted reward for the trajectory τ . Crucially,

this expectation is taken with respect to the initial state distribution and the sequence of independent noise variables sampled from the source distribution at each time step.

4 Reparameterization Flow Policy Optimization

In this section, we detail the proposed algorithm, Reparameterization Flow Policy. RFO comprises three key components. First, we derive the optimization of flow policies with RPG. Second, we introduce two regularization terms that are critical for RFO’s performance. Finally, we present a variant of RFO that incorporates an action chunking mechanism.

4.1 Reparameterization Policy Gradient for Flow Policy

We now detail the first key component of RFO: reparameterization policy gradient for flow policies. We adopt the *discretize-then-optimize* paradigm [34] for flow policy optimization, consistent with prior studies on reinforcement learning with flow policies [53, 29, 54, 13]. Specifically, given the neural-network-parameterized vector field v_θ , we perform numerical integration on the ODE using Euler method [1]. We employ the double-subscript notation $a_{t,k}$, where the subscript t denotes the MDP time step and k indexes the internal discrete integration steps. The generation process is formalized as follows:

$$\begin{aligned} a_{t,0} &= \epsilon_t, \quad \text{where } \epsilon_t \sim p_0, \\ a_{t,k+1} &= a_{t,k} + \Delta u \cdot v_\theta(a_{t,k}, u_k | s_t), \quad k = 0, \dots, K-1, \\ a_t &= a_{t,K}, \end{aligned} \tag{8}$$

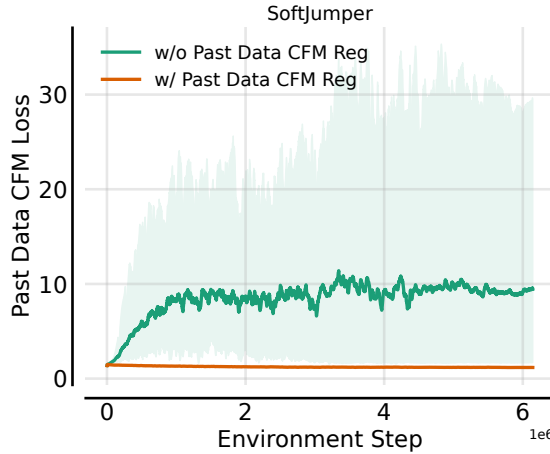
where $\Delta u = 1/K$ is the step size and $u_k = k \cdot \Delta u$ denotes the k -th flow time. Consequently, Euler integration process explicitly defines a differentiable transformation from the noise ϵ_t to the action a_t . We denote this transformation as $a_t = F_\theta(\epsilon_t; s_t)$. Based on this, we have the following key insight to optimize RFO:

Key Insight: Flow policies inherently parameterize a differentiable mapping from source noise to actions. This structure is naturally compatible with the Reparameterization Policy Gradient framework, enabling the computation of policy gradients via end-to-end backpropagation jointly through the environment dynamics and the flow policy.

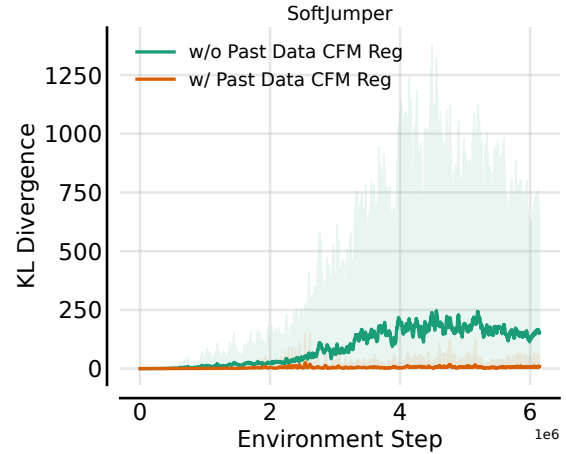
An illustration of this insight is shown in Figure 1. To formalize this insight, reparameterization policy gradient for the flow policy is expressed as:

$$\nabla_\theta J(\theta) = \mathbb{E}_{s_0, \epsilon_0, \epsilon_1, \dots} \left[\nabla_\theta \sum_{t=0}^{\infty} \gamma^t r(s_t, F_\theta(\epsilon_t; s_t)) \right], \tag{9}$$

where ϵ_t denotes the noise sampled from the source distribution at time t , and F_θ represents the flow transformation. The gradient is computed via backpropagation through time (BPTT) on the computational graph,



(a) Past Data CFM Loss



(b) KL Divergence

Figure 2: Comparison of RFO training with and without past data CFM regularization on the Soft Jumper task. We monitored the Conditional Flow Matching (CFM) loss of the current policy evaluated on actions sampled from the immediately preceding iteration, as well as the KL divergence between consecutive policy updates.

which includes both the flow ODE integration and the environment dynamics typically provided by a differentiable simulator or a learned world model.

In practice, backpropagating through long horizons can lead to exploding gradients. Therefore, we adopt the Short-Horizon Actor-Critic (SHAC) paradigm [49, 16] by truncating the trajectory into short segments. We define the short-horizon surrogate objective $\hat{J}(\theta)$ as:

$$\hat{J}(\theta) = \mathbb{E}_{s_0, \epsilon_0, \dots} \left[\sum_{t=0}^{H-1} \gamma^t r(s_t, F_\theta(\epsilon_t; s_t)) + \gamma^H V_\omega(s_H) \right]. \quad (10)$$

The gradient is thus *approximated* as:

$$\begin{aligned} \hat{\nabla}_\theta J(\theta) \\ = \mathbb{E} \left[\nabla_\theta \left(\sum_{t=0}^{H-1} \gamma^t r(s_t, F_\theta(\epsilon_t; s_t)) + \gamma^H V_\omega(s_H) \right) \right], \end{aligned} \quad (11)$$

where s_0 represents the start state of the current segment, $V_\omega(s_H)$ is the terminal value estimate to account for future rewards.

4.2 Regularization Terms

RFO incorporates two regularization terms that are crucial for performance. The first term addresses the stability of policy updates. RPG optimizes the policy by backpropagating gradients through the ODE integration steps, which can potentially disrupt the flow trajectories towards previously generated actions,

rendering them unlikely to be re-sampled under the updated policy.

To illustrate this phenomenon, we conducted experiments on the Soft Jumper task using the Rewarped simulator [48]. We monitored the Conditional Flow Matching (CFM) loss of the current policy evaluated on actions sampled from the immediately preceding iteration. As shown in Figure 2, the CFM loss steadily increases and remains high, indicating that the updated vector field struggles to reconstruct past actions. Furthermore, we tracked the KL divergence between consecutive policy updates (KL divergence approximation details are provided in Appendix E). The large KL divergence clearly signals training instability.

Hence, intuitively, we aim to regularize the vector field to retain paths from the source distribution to these recently sampled actions. We propose the *Past Data CFM Regularization*. This term treats the recent rollouts' actions as target samples and ensures the vector field points towards them. The objective $\mathcal{L}_{\text{past}}$ is defined as:

$$\begin{aligned} \mathcal{L}_{\text{past}}(\theta) \\ = \mathbb{E}_{\substack{u \sim \mathcal{U}[0,1], \epsilon \sim p_0, \\ (s,a) \sim \mathcal{D}_{\text{recent}}}} \left[\|v_\theta(\psi_u, u|s) - (a - \epsilon)\|^2 \right], \end{aligned} \quad (12)$$

where $\mathcal{D}_{\text{recent}}$ is a buffer including state-action pairs from the two most recent iterations (including the current iteration's rollout data), and u is the flow time. A discussion for the design of $\mathcal{D}_{\text{recent}}$ is in appendix F. Here, $\psi_u = (1 - u)\epsilon + ua$ represents the linear interpolation between the source noise ϵ and the target action a at flow time u . The effectiveness of $\mathcal{L}_{\text{past}}$ is empirically validated in our ablation study in Section 5.3. While self-imitation strategies have appeared in diffusion RL contexts [51], to the best of our knowledge, we are the first to uncover the distinct and fundamental role of Past Data CFM within the fundamentally different paradigm of RPG-driven flow policy optimization. Our analysis establishes that this regularization serves as a critical stabilizer for RPG-based flow optimization.

We introduce a second regularization term to explicitly promote exploration. Unlike prior Maximum Entropy approaches [14, 44, 8], which rely on approximating the entropy of the generative policy, we adopt a more direct strategy. Given the bounded action space in our setting, we leverage the property that maximizing entropy is equivalent to minimizing the KL divergence from a uniform distribution (see Example 12.2.4 in *Elements of Information Theory* [11]). Motivated by this, we propose to guide the flow policy toward uniformly sampled target actions via the CFM objective. While QVPO [12] explores a similar uniform-

Algorithm 1: Reparameterization Flow Policy Optimization (RFO)

- 1: Initialize θ, ω and buffers $\mathcal{D}_{\text{recent}}, \mathcal{D}_{\text{rollout}}$.
- 2: **for** iteration $k = 1, 2, \dots$ **do**
- 3: Collect short-horizon trajectories with flow policy; update $\mathcal{D}_{\text{recent}}$ and $\mathcal{D}_{\text{rollout}}$.
- 4: Compute RPG gradient for flow policy $\hat{\nabla} J$ via BPTT (Eq. equation 11).
- 5: Compute regularization CFM loss gradients $\nabla \mathcal{L}_{\text{past}}$ (Eq. equation 12) and $\nabla \mathcal{L}_{\text{uni}}$ (Eq. equation 13).
- 6: Update flow policy with combined and weighted gradients (Eq. equation 15).
- 7: Update critic ω for L epochs by minimizing Eq. equation 14.
- 8: **end for**

target regularization for diffusion policies, it employs state-dependent weighting. In contrast, we adopt a simple yet effective approach that treats all states encountered during rollouts equally. The proposed uniform exploration CFM objective, denoted as \mathcal{L}_{uni} , is defined as:

$$\begin{aligned} \mathcal{L}_{\text{uni}}(\theta) \\ = \mathbb{E}_{\substack{u \sim \mathcal{U}[0,1], \epsilon \sim p_0, \\ s \sim \mathcal{D}_{\text{rollout}}, a \sim p_{\text{uni}}}} \left[\|v_{\theta}(\psi_u, u | s) - (a - \epsilon)\|^2 \right], \end{aligned} \quad (13)$$

where $\mathcal{D}_{\text{rollout}}$ denotes the set of states visited during the current iteration's rollout, and p_{uni} represents the uniform distribution over the bounded action space. As before, ψ_u denotes the linear interpolation. The empirical effectiveness of \mathcal{L}_{uni} is analyzed in Section 5.3.

4.3 Value Function Training

We optimize the critic by minimizing the standard mean squared error loss [48, 49]:

$$\mathcal{L}(\omega) = \mathbb{E} [\|V_{\omega}(s) - y(s)\|^2], \quad (14)$$

where $y(s)$ denotes the TD- λ target [42]. Following the dual-critic architecture in SAPO [48], we calculate the target value by averaging the predictions of two separate critic networks.

4.4 Overall Policy Objective and RFO Algorithm

Combining the RPG objective for the flow policy (Eq. equation 11) with the past data CFM regularization (Eq. equation 12) and uniform exploration CFM regularization (Eq. equation 13), RFO minimizes the total policy loss:

$$\mathcal{L}_{\text{policy}}(\theta) = -\hat{J}(\theta) + c_{\text{past}}\mathcal{L}_{\text{past}}(\theta) + c_{\text{uni}}\mathcal{L}_{\text{uni}}(\theta), \quad (15)$$

where c_{past} and c_{uni} are hyperparameters weighting the stability and exploration regularization terms, respectively.

The overall RFO algorithm is described in Algorithm 1. We follow the SHAC paradigm, rolling out with flow policies to collect short-horizon trajectories. Then, we compute policy gradients and the gradients of the two CFM regularization terms. Combining and weighting these gradients, we update the policy. Afterwards, we update the value function by minimizing Eq. equation 14.

4.5 Action Chunking

Action chunking has proven beneficial for improving the temporal consistency of robot action generation [7], a critical factor in robotic applications. Therefore, we provide an extension to RFO that incorporates action chunking. In this variant, the flow policy predicts an action chunk of size C based on the current observation, encompassing both current and future actions. Subsequently, the agent executes these actions for C steps before replanning based on the new observation.

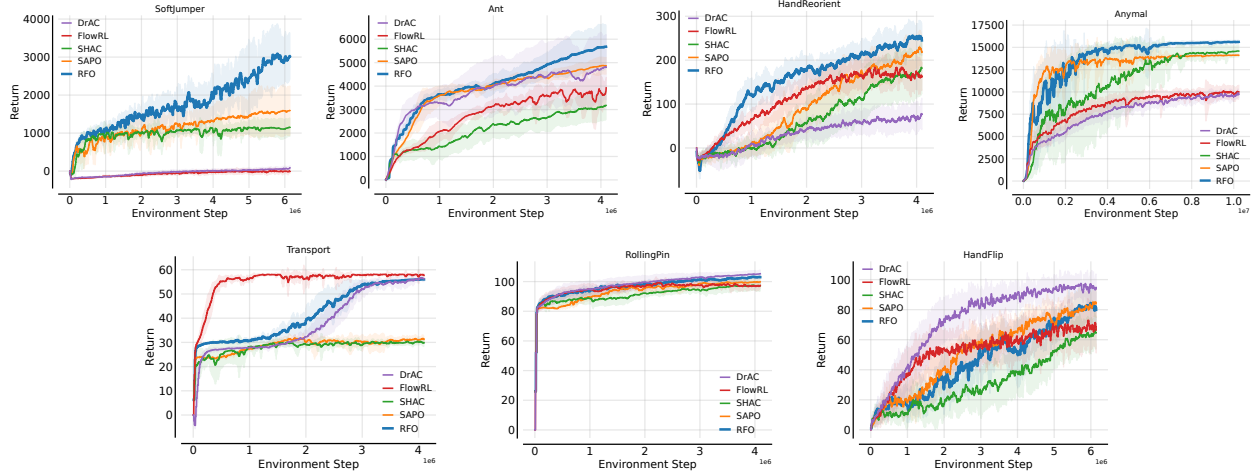


Figure 3: Training curves across seven tasks. Solid lines represent the mean return, while shaded regions indicate the standard deviation. Curves are smoothed using a 100-episode moving average.

5 Experiments

We conduct experiments to answer the following questions: **(i)** How does RFO’s performance compare to RPG-based approaches with Gaussian policies? **(ii)** How does RFO’s performance compare to other RL algorithms for flow or diffusion-based approaches? **(iii)** Are the two regularization terms critical to RFO’s performance? **(iv)** How does RFO work with the action chunking mechanism?

5.1 Experimental Setup

We evaluate our method on a comprehensive set of locomotion and manipulation tasks, utilizing either state or visual inputs within the differentiable simulators Rewarped [48] and DFlex [49, 16].

Tasks. Our experiments span diverse rigid and soft-body dynamics, categorized into:

- Locomotion tasks: Ant, ANYmal [21] (rigid quadruped), and Soft Jumper (visual soft body).
- Manipulation tasks: Hand Reorient (cube rotation), Rolling Pin (dough flattening), Hand Flip (object flipping), and Transport (liquid transport).

Visual inputs are used for Soft Jumper and the last three manipulation tasks.

Baselines. We compare RFO against strong baselines from two categories:

- RPG Baselines: SAPO [48] (SOTA RPG-based method with maximum entropy) and SHAC [49] (short-horizon RPG).
- Flow/Diffusion RL Baselines: DrAC [46] (a SOTA diffusion policy) and FlowRL [29] (a SOTA flow RL method).

All tasks are evaluated using at least 10 random seeds for each algorithm.

Table 1: Final performance evaluation after training. Results are reported as mean \pm standard deviation across all random seeds. Each seed is evaluated over 128 episodes. Normalized score = $\frac{\text{Mean Reward}}{\text{SHAC Mean Reward}}$.

(a) Raw Final Evaluation Rewards

Task	DrAC	FlowRL	SHAC	SAPO	RFO (Ours)
Soft Jumper	83.56 ± 67.60	-75.71 ± 139.54	1148.87 ± 233.84	1597.99 ± 653.87	3023.96 ± 603.61
Ant	4846.41 ± 1412.76	4083.45 ± 1082.79	3143.08 ± 569.50	4865.36 ± 363.77	5677.88 ± 964.49
Hand Reorient	73.74 ± 34.22	135.57 ± 39.34	174.63 ± 57.54	213.44 ± 33.95	258.84 ± 21.80
ANYmal	9554.46 ± 928.33	9717.58 ± 1619.35	14568.97 ± 652.72	14095.90 ± 82.02	15622.76 ± 200.87
Transport	57.07 ± 0.85	58.04 ± 0.19	30.00 ± 1.43	31.35 ± 1.24	56.00 ± 0.28
Rolling Pin	104.71 ± 2.00	92.49 ± 2.88	97.29 ± 3.44	99.79 ± 2.42	103.11 ± 1.26
Hand Flip	89.82 ± 4.59	54.80 ± 18.55	65.57 ± 11.75	83.00 ± 7.49	82.65 ± 11.65

(b) SHAC-normalized Final Evaluation Rewards

Task	DrAC	FlowRL	SHAC	SAPO	RFO (Ours)
Soft Jumper	0.07 ± 0.06	-0.07 ± 0.12	1.00 ± 0.20	1.39 ± 0.57	2.63 ± 0.53
Ant	1.54 ± 0.45	1.30 ± 0.34	1.00 ± 0.18	1.55 ± 0.12	1.81 ± 0.31
Hand Reorient	0.42 ± 0.20	0.78 ± 0.23	1.00 ± 0.33	1.22 ± 0.19	1.48 ± 0.12
ANYmal	0.66 ± 0.06	0.67 ± 0.11	1.00 ± 0.04	0.97 ± 0.01	1.07 ± 0.01
Transport	1.90 ± 0.03	1.93 ± 0.01	1.00 ± 0.05	1.05 ± 0.04	1.87 ± 0.01
Rolling Pin	1.08 ± 0.02	0.95 ± 0.03	1.00 ± 0.04	1.03 ± 0.02	1.06 ± 0.01
Hand Flip	1.37 ± 0.07	0.84 ± 0.28	1.00 ± 0.18	1.27 ± 0.11	1.26 ± 0.18
Average	1.01	0.91	1.00	1.21	1.60

5.2 Main Experiment Results

We show the training curves in Figure 3 and final performance evaluation results in Table 1.

In the Soft Jumper, Ant, ANYmal, and Hand Reorient tasks, RFO outperforms all baselines by substantial margins. Most notably, in the Soft Jumper task, RFO achieves a final reward nearly $2\times$ that of the best baseline, underscoring its capability in high-dimensional control settings (action space \mathbb{R}^{222}). This superiority extends to rigid-body dynamics, where RFO consistently dominates strong baselines, securing performance gains of approximately 21% on Hand Reorient and 17% on Ant, while boosting the reward by over 1000 points on the ANYmal task. Furthermore, RFO demonstrates remarkable robustness on the Rolling Pin and Transport tasks, achieving performance comparable to the state-of-the-art with marginal gaps of only 1.5% and 3.5%, respectively. As shown in the aggregate performance analysis (Table 1 (b)), which normalizes scores against the SHAC baseline, RFO delivers superior overall performance across the diverse task suite.

From the RPG perspective, RFO consistently improves upon SHAC and SAPO, validating the efficacy of integrating flow policies into the RPG framework. Compared to Flow and Diffusion baselines, RFO demonstrates a clear advantage by leveraging analytical gradients from RPG. This becomes particularly evident in the Soft Jumper, ANYmal, and Hand Reorient tasks, where DrAC and FlowRL struggle, while RFO demonstrates superior performance. Additionally, DrAC requires 20 denoising steps for action sampling,

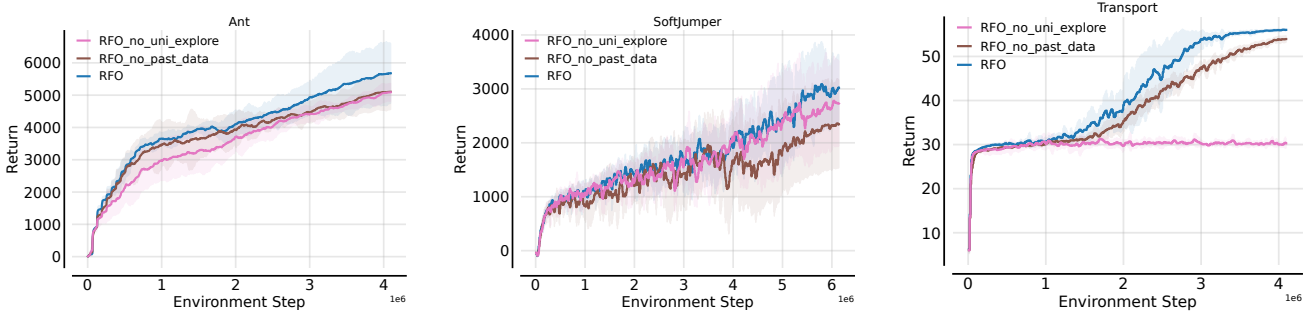


Figure 4: Ablation study for the effectiveness of past data CFM regularization and uniform exploration CFM regularization. The results show that the two proposed regularization terms are critical for RFO’s performance.

which not only slows down inference but also significantly increases training time compared to RFO, since it needs to backpropagate through all 20 action generation steps. Furthermore, despite being an on-policy algorithm, RFO achieves sample efficiency comparable to off-policy flow-based methods thanks to RPG, while avoiding the need to approximate intractable action log-likelihoods.

5.3 Ablation Study

In this section, we conduct ablation experiments to answer the following questions: **(i)** Are the two proposed regularization terms, past data CFM regularization and uniform exploration CFM regularization, critical for RFO’s performance? **(ii)** How does RFO perform under a range of hyperparameters, including the weights for the two CFM objectives and the number of flow integration steps?

To answer the first question, we conduct experiments on the Ant, Soft Jumper, and Transport tasks. We compare the full RFO algorithm against two variants: RFO without past data CFM regularization and RFO without uniform exploration CFM regularization. The training curves are presented in Figure 4.

Without past data CFM regularization, RFO’s performance significantly degrades across all three tasks, suggesting that this term is crucial for both training stability and final performance. Similarly, removing the uniform exploration regularization leads to performance drops across all tasks. Most notably, on the Transport task, omitting uniform exploration regularization causes RFO’s performance to degrade to the levels of SHAC and SAPO, clearly highlighting the effectiveness of the uniform random exploration strategy.

To answer the second question, we conduct experiments on the Soft Jumper task. We evaluate RFO with different combinations of c_{past} and c_{uni} , which control the weights of the two regularization terms. We also evaluate RFO with varying numbers of flow Euler integration steps. The training curves are provided in Appendix C, demonstrating that RFO exhibits strong robustness across a wide range of hyperparameters.

5.4 Action Chunking Results

Figure 6 in Appendix D illustrates the training curves for RFO with action chunking across the evaluated tasks. This result is particularly encouraging given the inherent challenge: the flow policy must predict

action sequences for future time steps based solely on the current observation, without the guidance of expert data used in imitation learning. Such optimization is harder, as the policy must generate valid future actions without access to the corresponding intermediate states. Consequently, this setup suggests that integrating offline-to-online procedures could be a promising direction to further enhance RPG-based flow policies.

6 Conclusion

In this work, we introduce Reparameterization Flow Policy Optimization, a novel framework that bridges the gap between flow-based generative policies and the high sample efficiency of Reparameterization Policy Gradients. By integrating tailored regularization terms for training stability and exploration, RFO achieves strong performance. Empirical evaluations across diverse rigid and soft-body control tasks demonstrate that RFO achieves SOTA performance. We further explored an action-chunking RFO variant. Future directions include extending RFO to offline-to-online reinforcement learning settings.

References

- [1] *Numerical Differential Equation Methods*, chapter 2, pages 55–142. John Wiley & Sons, Ltd, 2016.
- [2] Tara Akhoud-Sadegh, Jarid Rector-Brooks, Avishek Joey Bose, Sarthak Mittal, Pablo Lemos, Cheng-Hao Liu, Marcin Sendera, Siamak Ravanbakhsh, Gauthier Gidel, Yoshua Bengio, Nikolay Malkin, and Alexander Tong. Iterated denoising energy matching for sampling from boltzmann densities. In *Proceedings of the 41st International Conference on Machine Learning*, ICML’24. JMLR.org, 2024.
- [3] Michael Samuel Albergo and Eric Vanden-Eijnden. Building normalizing flows with stochastic interpolants. In *The Eleventh International Conference on Learning Representations*, 2023.
- [4] Brandon Amos, Samuel Stanton, Denis Yarats, and Andrew Gordon Wilson. On the model-based stochastic value gradient for continuous reinforcement learning. In Ali Jadbabaie, John Lygeros, George J. Pappas, Pablo A. Parrilo, Benjamin Recht, Claire J. Tomlin, and Melanie N. Zeilinger, editors, *Proceedings of the 3rd Conference on Learning for Dynamics and Control*, volume 144 of *Proceedings of Machine Learning Research*, pages 6–20. PMLR, 07 – 08 June 2021.
- [5] Kevin Black, Noah Brown, James Darpinian, Karan Dhabalia, Danny Driess, Adnan Esmail, Michael Robert Equi, Chelsea Finn, Niccolo Fusai, Manuel Y. Galliker, Dibya Ghosh, Lachy Groom, Karol Hausman, brian ichter, Szymon Jakubczak, Tim Jones, Liyiming Ke, Devin LeBlanc, Sergey Levine, Adrian Li-Bell, Mohith Mothukuri, Suraj Nair, Karl Pertsch, Allen Z. Ren, Lucy Xiaoyang Shi, Laura Smith, Jost Tobias Springenberg, Kyle Stachowicz, James Tanner, Quan Vuong, Homer Walke, Anna Walling, Haohuan Wang, Lili Yu, and Ury Zhilinsky. $\pi_{0.5}$: a vision-language-action model with open-world generalization. In Joseph Lim, Shuran Song, and Hae-Won Park, editors, *Proceedings of The 9th Conference on Robot Learning*, volume 305 of *Proceedings of Machine Learning Research*, pages 17–40. PMLR, 27–30 Sep 2025.

- [6] Kevin Black, Noah Brown, Danny Driess, Adnan Esmail, Michael Equi, Chelsea Finn, Niccolo Fusai, Lachy Groom, Karol Hausman, Brian Ichter, Szymon Jakubczak, Tim Jones, Liyiming Ke, Sergey Levine, Adrian Li-Bell, Mohith Mothukuri, Suraj Nair, Karl Pertsch, Lucy Xiaoyang Shi, James Tanner, Quan Vuong, Anna Walling, Haohuan Wang, and Ury Zhilinsky. π_0 : A vision-language-action flow model for general robot control, 2026.
- [7] Kevin Black, Manuel Y Galliker, and Sergey Levine. Real-time execution of action chunking flow policies. In *The Thirty-ninth Annual Conference on Neural Information Processing Systems*, 2025.
- [8] Onur Celik, Zechu Li, Denis Blessing, Ge Li, Daniel Palenicek, Jan Peters, Georgia Chalvatzaki, and Gerhard Neumann. DIME: Diffusion-based maximum entropy reinforcement learning. In *Forty-second International Conference on Machine Learning*, 2025.
- [9] Ricky T. Q. Chen, Yulia Rubanova, Jesse Bettencourt, and David K Duvenaud. Neural ordinary differential equations. In S. Bengio, H. Wallach, H. Larochelle, K. Grauman, N. Cesa-Bianchi, and R. Garnett, editors, *Advances in Neural Information Processing Systems*, volume 31. Curran Associates, Inc., 2018.
- [10] Tianyi Chen, Haitong Ma, Na Li, Kai Wang, and Bo Dai. One-step flow policy mirror descent, 2025.
- [11] Thomas M Cover. *Elements of information theory*. John Wiley & Sons, 1999.
- [12] Shutong Ding, Ke Hu, Zhenhao Zhang, Kan Ren, Weinan Zhang, Jingyi Yu, Jingya Wang, and Ye Shi. Diffusion-based reinforcement learning via q-weighted variational policy optimization. In *The Thirty-eighth Annual Conference on Neural Information Processing Systems*, 2024.
- [13] Shutong Ding, Ke Hu, Shan Zhong, Haoyang Luo, Weinan Zhang, Jingya Wang, Jun Wang, and Ye Shi. GenPO: Generative diffusion models meet on-policy reinforcement learning. In *The Thirty-ninth Annual Conference on Neural Information Processing Systems*, 2025.
- [14] Xiaoyi Dong, Jian Cheng, and Xi Sheryl Zhang. Maximum entropy reinforcement learning with diffusion policy. In *Forty-second International Conference on Machine Learning*, 2025.
- [15] Feng Gao, Liangzhi Shi, Shenao Zhang, Zhaoran Wang, and Yi Wu. Adaptive-gradient policy optimization: Enhancing policy learning in non-smooth differentiable simulations. In *Forty-first International Conference on Machine Learning*, 2024.
- [16] Ignat Georgiev, Krishnan Srinivasan, Jie Xu, Eric Heiden, and Animesh Garg. Adaptive horizon actor-critic for policy learning in contact-rich differentiable simulation. In *Proceedings of the 41st International Conference on Machine Learning*, ICML’24. JMLR.org, 2024.
- [17] Danijar Hafner, Timothy Lillicrap, Jimmy Ba, and Mohammad Norouzi. Dream to control: Learning behaviors by latent imagination. In *International Conference on Learning Representations*, 2020.

[18] Johannes Heeg, Yunlong Song, and Davide Scaramuzza. Learning quadrotor control from visual features using differentiable simulation. In *2025 IEEE International Conference on Robotics and Automation (ICRA)*, pages 4033–4039, 2025.

[19] Yuanming Hu, Luke Anderson, Tzu-Mao Li, Qi Sun, Nathan Carr, Jonathan Ragan-Kelley, and Frédo Durand. DiffTaichi: Differentiable programming for physical simulation. *ICLR*, 2020.

[20] Zhiao Huang, Litian Liang, Zhan Ling, Xuanlin Li, Chuang Gan, and Hao Su. Reparameterized policy learning for multimodal trajectory optimization. In *Proceedings of the 40th International Conference on Machine Learning*, ICML’23. JMLR.org, 2023.

[21] M. Hutter, C. Gehring, A. Lauber, F. Gunther, C. D. Bellicoso, V. Tsounis, P. Fankhauser, R. Diethelm, S. Bachmann, M. Bloesch, H. Kolenbach, M. Bjelonic, L. Isler, and K. Meyer and. Anymal - toward legged robots for harsh environments. *Advanced Robotics*, 31(17):918–931, 2017.

[22] Physical Intelligence, Ali Amin, Raichelle Aniceto, Ashwin Balakrishna, Kevin Black, Ken Conley, Grace Connors, James Darpinian, Karan Dhabalia, Jared DiCarlo, Danny Driess, Michael Equi, Adnan Esmail, Yunhao Fang, Chelsea Finn, Catherine Glossop, Thomas Godden, Ivan Goryachev, Lachy Groom, Hunter Hancock, Karol Hausman, Gashon Hussein, Brian Ichter, Szymon Jakubczak, Rowan Jen, Tim Jones, Ben Katz, Liyiming Ke, Chandra Kuchi, Marinda Lamb, Devin LeBlanc, Sergey Levine, Adrian Li-Bell, Yao Lu, Vishnu Mano, Mohith Mothukuri, Suraj Nair, Karl Pertsch, Allen Z. Ren, Charvi Sharma, Lucy Xiaoyang Shi, Laura Smith, Jost Tobias Springenberg, Kyle Stachowicz, Will Stoeckle, Alex Swerdlow, James Tanner, Marcel Torne, Quan Vuong, Anna Walling, Haohuan Wang, Blake Williams, Sukwon Yoo, Lili Yu, Ury Zhilinsky, and Zhiyuan Zhou. $\pi_{0.6}^*$: a vla that learns from experience, 2025.

[23] Diederik P Kingma and Max Welling. Auto-encoding variational Bayes. In *International Conference on Learning Representations (ICLR)*, 2014.

[24] Chenhao Li, Andreas Krause, and Marco Hutter. Robotic world model: A neural network simulator for robust policy optimization in robotics. *arXiv preprint arXiv:2501.10100*, 2025.

[25] Qiyang Li, Zhiyuan Zhou, and Sergey Levine. Reinforcement learning with action chunking. In *The Thirty-ninth Annual Conference on Neural Information Processing Systems*, 2025.

[26] Yaron Lipman, Ricky T. Q. Chen, Heli Ben-Hamu, Maximilian Nickel, and Matthew Le. Flow matching for generative modeling. In *The Eleventh International Conference on Learning Representations*, 2023.

[27] Xingchao Liu, Chengyue Gong, and qiang liu. Flow straight and fast: Learning to generate and transfer data with rectified flow. In *The Eleventh International Conference on Learning Representations*, 2023.

[28] Jing Yuan Luo, Yunlong Song, Victor Klemm, Fan Shi, Davide Scaramuzza, and Marco Hutter. Residual policy learning for perceptive quadruped control using differentiable simulation. In *2025 IEEE International Conference on Robotics and Automation (ICRA)*, pages 1–8, 2025.

[29] Lei Lv, Yunfei Li, Yu Luo, Fuchun Sun, Tao Kong, Jiafeng Xu, and Xiao Ma. Flow-based policy for on-line reinforcement learning. In *The Thirty-ninth Annual Conference on Neural Information Processing Systems*, 2025.

[30] Haitong Ma, Tianyi Chen, Kai Wang, Na Li, and Bo Dai. Efficient online reinforcement learning for diffusion policy. In *Forty-second International Conference on Machine Learning*, 2025.

[31] David McAllister, Songwei Ge, Brent Yi, Chung Min Kim, Ethan Weber, Hongsuk Choi, Haiwen Feng, and Angjoo Kanazawa. Flow matching policy gradients, 2025.

[32] Shakir Mohamed, Mihaela Rosca, Michael Figurnov, and Andriy Mnih. Monte carlo gradient estimation in machine learning. *J. Mach. Learn. Res.*, 21(1), January 2020.

[33] NVIDIA, :, Mayank Mittal, Pascal Roth, James Tigue, Antoine Richard, Octi Zhang, Peter Du, Antonio Serrano-Muñoz, Xinjie Yao, René Zurbrügg, Nikita Rudin, Lukasz Wawrzyniak, Milad Rakhsha, Alain Denzler, Eric Heiden, Ales Borovicka, Ossama Ahmed, Iretiayo Akinola, Abrar Anwar, Mark T. Carlson, Ji Yuan Feng, Animesh Garg, Renato Gasoto, Lionel Gulich, Yijie Guo, M. Gussert, Alex Hansen, Mihir Kulkarni, Chenran Li, Wei Liu, Viktor Makoviychuk, Grzegorz Malczyk, Hammad Mazhar, Massoud Moghani, Adithyavairavan Murali, Michael Noseworthy, Alexander Poddubny, Nathan Ratliff, Welf Rehberg, Clemens Schwarke, Ritvik Singh, James Latham Smith, Bingjie Tang, Ruchik Thaker, Matthew Trepte, Karl Van Wyk, Fangzhou Yu, Alex Millane, Vikram Ramasamy, Remo Steiner, Sangeeta Subramanian, Clemens Volk, CY Chen, Neel Jawale, Ashwin Varghese Kuruttukulam, Michael A. Lin, Ajay Mandlekar, Karsten Patzwaldt, John Welsh, Huihua Zhao, Fatima Anes, Jean-Francois Lafleche, Nicolas Moënne-Loccoz, Soowan Park, Rob Stepinski, Dirk Van Gelder, Chris Amevor, Jan Carius, Jumyung Chang, Anka He Chen, Pablo de Heras Ciechomski, Gilles Daviet, Mohammad Mohajerani, Julia von Muralt, Viktor Reutskyy, Michael Sauter, Simon Schirm, Eric L. Shi, Pierre Terdiman, Kenny Vilella, Tobias Widmer, Gordon Yeoman, Tiffany Chen, Sergey Grizan, Cathy Li, Lotus Li, Connor Smith, Rafael Wiltz, Kostas Alexis, Yan Chang, David Chu, Linxi "Jim" Fan, Farbod Farshidian, Ankur Handa, Spencer Huang, Marco Hutter, Yashraj Narang, Soha Pouya, Shiwei Sheng, Yuke Zhu, Miles Macklin, Adam Moravanszky, Philipp Reist, Yunrong Guo, David Hoeller, and Gavriel State. Isaac lab: A gpu-accelerated simulation framework for multi-modal robot learning, 2025.

[34] Derek Onken and Lars Ruthotto. Discretize-optimize vs. optimize-discretize for time-series regression and continuous normalizing flows, 2020.

[35] Jiahe Pan, Jiaxu Xing, Rudolf Reiter, Yifan Zhai, Elie Aljalbout, and Davide Scaramuzza. Learning on the fly: Rapid policy adaptation via differentiable simulation. *IEEE Robotics and Automation Letters*, 2025.

[36] Seohong Park, Qiyang Li, and Sergey Levine. Flow q-learning. In *International Conference on Machine Learning (ICML)*, 2025.

[37] Michael Psenka, Alejandro Escontrela, Pieter Abbeel, and Yi Ma. Learning a diffusion model policy from rewards via q-score matching. In *Proceedings of the 41st International Conference on Machine Learning*, ICML'24. JMLR.org, 2024.

[38] Allen Z. Ren, Justin Lidard, Lars Lien Ankile, Anthony Simeonov, Pulkit Agrawal, Anirudha Majumdar, Benjamin Burchfiel, Hongkai Dai, and Max Simchowitz. Diffusion policy policy optimization. In *The Thirteenth International Conference on Learning Representations*, 2025.

[39] Danilo Jimenez Rezende, Shakir Mohamed, and Daan Wierstra. Stochastic backpropagation and approximate inference in deep generative models. In *Proceedings of The 30th International Conference on Machine Learning (ICML)*, 2014.

[40] John Schulman. Approximating KL divergence, 2020. <http://joschu.net/blog/kl-approx.html>.

[41] Clemens Schwarke, Victor Klemm, Joshua Bagajo, Jean Pierre Sleiman, Ignat Georgiev, Jesus Torde-sillas Torres, and Marco Hutter. Learning deployable locomotion control via differentiable simulation. In *9th Annual Conference on Robot Learning*, 2025.

[42] Richard S. Sutton and Andrew G. Barto. *Reinforcement Learning: An Introduction*. A Bradford Book, Cambridge, MA, USA, 2018.

[43] Richard S Sutton, David McAllester, Satinder Singh, and Yishay Mansour. Policy gradient methods for reinforcement learning with function approximation. In S. Solla, T. Leen, and K. Müller, editors, *Advances in Neural Information Processing Systems*, volume 12. MIT Press, 1999.

[44] Yinuo Wang, Likun Wang, Yuxuan Jiang, Wenjun Zou, Tong Liu, Xujie Song, Wenxuan Wang, Liming Xiao, Jiang WU, Jingliang Duan, and Shengbo Eben Li. Diffusion actor-critic with entropy regulator. In *The Thirty-eighth Annual Conference on Neural Information Processing Systems*, 2024.

[45] Yinuo Wang, Likun Wang, Mining Tan, Wenjun Zou, Xujie Song, Wenxuan Wang, Tong Liu, Guojian Zhan, Tianze Zhu, Shiqi Liu, Zeyu He, Feihong Zhang, Jingliang Duan, and Shengbo Eben Li. Enhanced dacer algorithm with high diffusion efficiency, 2025.

[46] Ziqi Wang, Jiashun Liu, and Ling Pan. Learning intractable multimodal policies with reparameterization and diversity regularization. In *Annual Conference on Neural Information Processing Systems*, 2025.

[47] Ronald J Williams. Simple statistical gradient-following algorithms for connectionist reinforcement learning. *Machine learning*, 8:229–256, 1992.

[48] Eliot Xing, Vernon Luk, and Jean Oh. Stabilizing reinforcement learning in differentiable multiphysics simulation. In *The Thirteenth International Conference on Learning Representations*, 2025.

[49] Jie Xu, Viktor Makoviychuk, Yashraj Narang, Fabio Ramos, Wojciech Matusik, Animesh Garg, and Miles Macklin. Accelerated policy learning with parallel differentiable simulation. In *International Conference on Learning Representations*, 2021.

- [50] Long Yang, Zhixiong Huang, Fenghao Lei, Yucun Zhong, Yiming Yang, Cong Fang, Shiting Wen, Binbin Zhou, and Zhouchen Lin. Policy representation via diffusion probability model for reinforcement learning, 2023.
- [51] Ningyuan Yang, Jiaxuan Gao, Feng Gao, Yi Wu, and Chao Yu. Fine-tuning diffusion policies with backpropagation through diffusion timesteps, 2025.
- [52] Chubin Zhang, Zhenglin Wan, Feng Chen, Xingrui Yu, Ivor Tsang, and Bo An. Gorl: An algorithm-agnostic framework for online reinforcement learning with generative policies, 2025.
- [53] Tonghe Zhang, Chao Yu, Sichang Su, and Yu Wang. Reinflow: Fine-tuning flow matching policy with online reinforcement learning. In *The Thirty-ninth Annual Conference on Neural Information Processing Systems*, 2025.
- [54] Yixian Zhang, Shu'ang Yu, Tonghe Zhang, Mo Guang, Haojia Hui, Kaiwen Long, Yu Wang, Chao Yu, and Wenbo Ding. Sac flow: Sample-efficient reinforcement learning of flow-based policies via velocity-reparameterized sequential modeling, 2025.
- [55] Yuang Zhang, Yu Hu, Yunlong Song, Danping Zou, and Weiyao Lin. Learning vision-based agile flight via differentiable physics. *Nature Machine Intelligence*, pages 1–13, 2025.
- [56] Hai Zhong, Xun Wang, Zhuoran Li, and Longbo Huang. Reparameterization proximal policy optimization, 2025.

A Task Details

We conduct experiments with two differentiable physics simulators: DFlex [49, 16] from NVIDIA and Rewarped [48]. More specifically, we use AHAC’s version of the DFlex simulator and Rewarped version 1.3.0 from <https://github.com/rewarded/rewarded>.

Here, we provide details of the tasks used in the main experiments.

A.1 Ant

Ant is a classical locomotion task using the Rewarped simulator [48], where the goal is to maximize forward velocity. Ant uses state inputs. The state space is R^{37} and the action space is R^8 , including joint torques [48].

A.2 Hand Reorient

Hand Reorient is a task from Rewarped [48], where the goal is to reorient a cube with an Allegro dexterous hand, using state inputs. The state space is R^{72} and the action space is R^{16} , including joint torques [48].

A.3 Rolling Pin

Rolling Pin is a manipulation task from Rewarped [48], where the goal is to flatten dough with a rolling pin, using pixel inputs. The observation space consists of $[R^{250 \times 3}, R^3, R^3]$, and the action space is R^3 , including relative position and orientation [48].

A.4 Soft Jumper

Soft Jumper is a soft-body locomotion task from Rewarped [48] with pixel inputs. The observation space consists of $[R^{204 \times 3}, R^3, R^3, R^{222}]$, and the action space is R^{222} , including tetrahedral activations [48].

A.5 Hand Flip

Hand Flip is a soft-object manipulation task from Rewarped [48] using a Shadow Hand and pixel inputs. The observation space consists of $[R^{250 \times 3}, R^3, R^{24}]$, and the action space is R^{24} , including relative position and orientation [48].

A.6 Transport

Transport is a soft-object manipulation task from Rewarped [48] with pixel inputs. The observation space consists of $[R^{250 \times 3}, R^3, R^3, R^3]$, and the action space is R^3 , including relative position [48].

A.7 ANYmal

ANYmal is a locomotion task from DFLEX [16] with state inputs, where the goal is to maximize the forward velocity of a quadruped robot [21]. The state space is R^{49} and the action space is R^{12} .

B Baselines, Implementation Details and Hyperparameter

B.1 Baselines and Hyperparameters

We benchmark RFO against four baselines: SHAC [49], SAPO [48], DrAC [46], and FlowRL [29]. For SAPO, we utilize the official repository¹, from which we also adopt the improved SHAC implementation as it demonstrates improved and stable performance. For DrAC (Diffusion Policy) and FlowRL (Flow Policy), we adapt their official implementations to support parallelized environments and incorporate visual encoders for pixel-based inputs. We use their default sampler and integration steps for action sampling.

We tune the hyperparameters of DrAC and FlowRL individually for each task, finding that the Update-to-Data (UTD) ratio affects their performance significantly (FlowRL defaults to 0.5, as in their official repository). Note that tuning DrAC with UTD ratios ≥ 1 is computationally prohibitive, as training would require weeks to complete. Furthermore, we observe that a higher UTD ratio does not necessarily translate to better performance. We align the neural network sizes across all algorithms. For visual input tasks, we use DP3 Point Net with layers [64, 128, 256] and 64-dimension output, average pooling for all algorithms. Shared hyperparameters are detailed in Table 2.

Table 2: Common hyperparameters for all algorithms.

	shared	RFO	SHAC	SAPO	DrAC	FlowRL
Horizon H	32					
Epochs for critics L		16	16	16	see UTD ratio	see UTD ratio
Epochs for actors M		1	1	1	see UTD ratio	see UTD ratio
Discount γ	0.99					
TD/GAE λ	0.95				N.A.	N.A.
Actor MLP	(400, 200, 100)					
Critic MLP	(400, 200, 100)					
Actor η		$2e - 3$	$2e - 3$	$2e - 3$	$3e - 4$	$3e - 4$
Critic η	$5e - 4$				$3e - 4$	$3e - 4$
Learning rate schedule	-	linear	linear	linear	N.A.	N.A.
Optim type	AdamW					
Optim (β_1, β_2)	(0.7, 0.95)	(0.9, 0.999)	(0.9, 0.999)	(0.9, 0.999)		
Norm type	LayerNorm					
Activation type	SiLU					

¹<https://github.com/etaoxing/mineral>

Table 3: The number of parallel environments used for each environment. These values are kept the same as in the official implementations: we follow the AHAC repository (<https://github.com/imgeorgiev/DiffRL>) for the DFlex tasks and the Rewarped repository.

	Ant	Transport	Hand Flip	Rolling Pin	Soft Jumper	Anymal	Hand Reorient
Num Envs	64	32	32	32	32	128	64

Table 4: UTD ratios for FlowRL and DrAC.

	Ant	Transport	Hand Flip	Rolling Pin	Soft Jumper	Anymal	Hand Reorient
DrAC	0.5	0.125	0.5	0.25	0.125	0.25	0.125
FlowRL	0.125	0.125	0.25	0.5	0.5	0.25	0.25

B.2 Implementation Details of RFO

Since the flow velocity field can generate unbounded actions, we apply a \tanh squashing function to the output. We utilize the pre- \tanh values as targets for both past data CFM regularization and uniform CFM regularization (although we found that using \tanh -transformed actions as targets is also effective). Additionally, we observe that excessively large pre- \tanh targets can cause issues for the CFM loss; hence, we apply clamping to bound them. Detailed unique hyperparameters for RFO are shown in Table 5.

Table 5: RFO’s unique hyperparameters.

	Ant	Transport	Hand Flip	Rolling Pin	Soft Jumper	Anymal	Hand Reorient
c_{past}	0.2	0.1	5e-4	5e-3	0.4	0.1	0.2
c_{uni}	0.2	0.1	0.2	5e-3	0.4	0.1	0.01

C Sensitivity to Hyperparameters

In this section, we conduct ablation experiments on: (i) different weight combinations for past data CFM regularization and uniform exploration CFM regularization, and (ii) the number of flow integration steps (RFO uses 4 flow steps across all tasks by default). As shown in Figure 5, RFO demonstrates robust performance across a wide range of hyperparameters.

D RFO with Action Chunking Results

Figure 6 illustrates the training curves for RFO augmented with the action chunking mechanism. We observe that RFO with action chunking generally maintains strong performance, largely matching that of the standard RFO baseline (without chunking) across the majority of evaluated environments. Although a minor performance degradation is observed in certain task, the results remain competitive. This is expected, as the flow policy is required to predict a sequence of actions simultaneously, which increases the complexity of

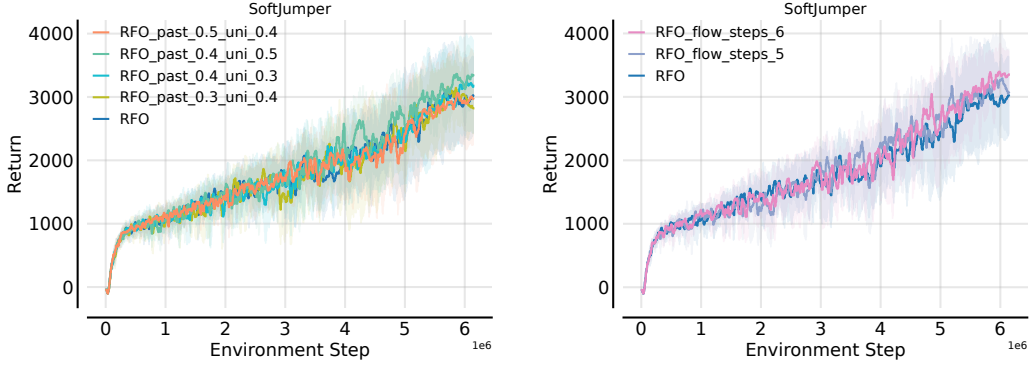


Figure 5: (a) Ablation study on different weight combinations for past data CFM regularization and uniform exploration CFM regularization. (b) Ablation study on the number of flow integration steps.

policy optimization.

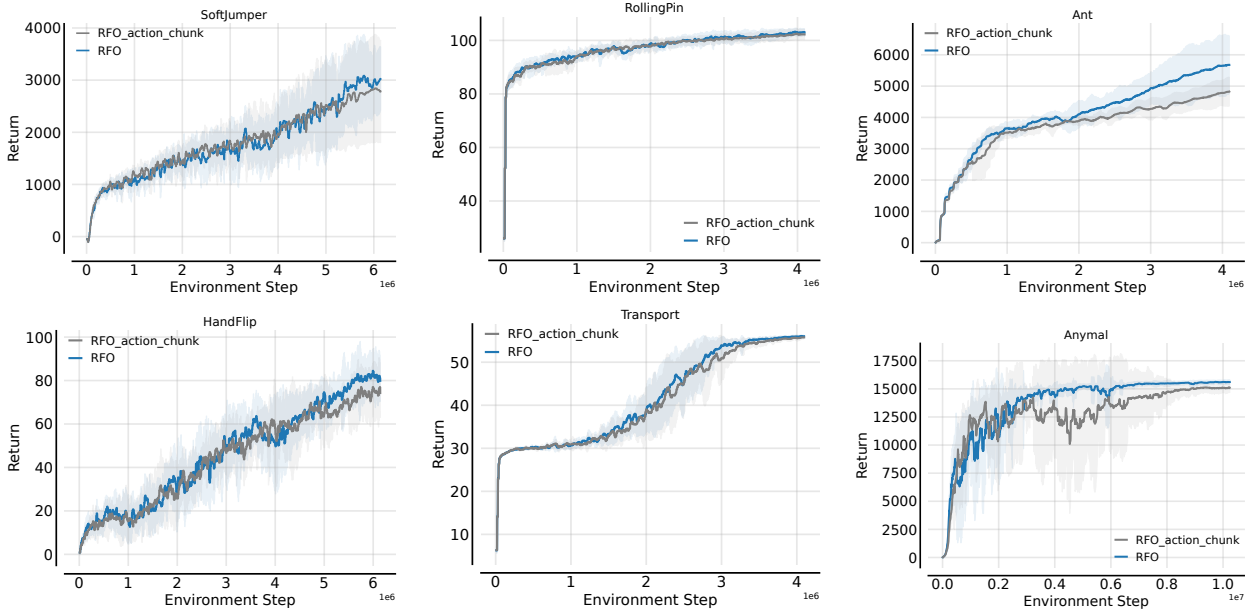


Figure 6: Training curves of RFO with the action chunking mechanism.

E Details of KL Divergence Estimation

In this section, we detail the approximation of the KL divergence between consecutive policy updates on the Soft Jumper task. Following the methodology in FPO [31], for a given state-action pair (s, a) and flow policies π_θ and $\pi_{\theta'}$, we can approximate the likelihood ratio $\frac{\pi_\theta(a|s)}{\pi_{\theta'}(a|s)}$ using the difference in their Conditional Flow Matching (CFM) losses. Specifically, this ratio is approximated as $\exp(L_{\theta'}^{\text{CFM}}(a|s) - L_\theta^{\text{CFM}}(a|s))$. Leveraging this relationship, we sample actions from the old/behavior policy π_θ and compute the CFM losses for both π_θ and $\pi_{\theta'}$ using these samples as targets. Finally, we employ the K3 estimator [40] to estimate the KL divergence $\text{KL}(\pi_\theta \parallel \pi_{\theta'})$.

F Design Choice

In this section, we justify our decision to include rollout states and actions from both the current and previous iterations in $\mathcal{D}_{\text{recent}}$. As shown in Figure 7, relying solely on the current iteration results in significantly slower learning. Conversely, using data from three iterations leads to degraded performance and reduced learning speed. In contrast, we find that including state-action pairs from both the current and previous iterations yields the best results in terms of final performance and convergence speed.

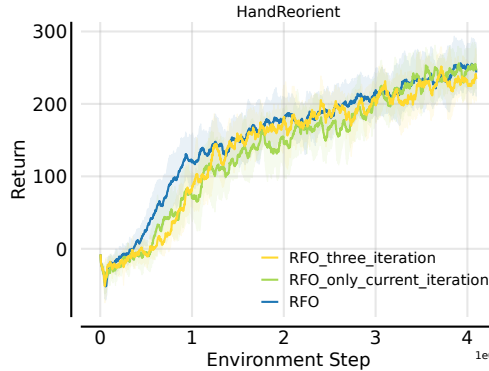


Figure 7: Comparison of $\mathcal{D}_{\text{recent}}$ including data from: the current iteration only, the current + previous iterations, and three iterations of rollout data.